Journal of the
Nigerian Mathematical Society
Vol. 40, Issue 3, pp. 301-320, 2021

THERMPHORETIC ANALYSIS AND NON-UNIFORM HEAT SOURCE IN HYDROMAGNETIC MICROPOLAR FLUID FLOW PASSING AN INCLINDED SHEET IN A POROUS MEDIUM

E. O. FATUNMBI, S. O. SALAWU[1] AND J. O. AJILORE

ABSTRACT. The investigation of heat and mass transfer engaging micropolar fluid is applicable in biomedical and engineering activities such as in blood flows, fluid flow in brain and porous pipe design. This research work reports on thermophoretic and non-uniform heat source in hydromagnetic micropolar fluid flow passing an inclined sheet in porous media and viscous dissipation. The work is analyzed based on the assumption of two-dimensional, steady, viscous, incompressible flow through inclined porous media sheet with the impact of uniform external magnetic field. Similarity conversion approach has been adopted to simplify the modelled equations and then solved numerically by means of shooting scheme together with integrating Fehlberg-Runge-Kutta algorithm in company of shooting techniques. Various graphs have been sketched while tables are constructed to highlight and discuss the impact of the main controlling parameters influencing the flow, thermal and solutal fields. Besides, the current results depict a strong relationship with previously published works in the literature under limiting situations. It is found that the impact of thermophoretic reactive micropolar fluid is to enhance mass transfer, velocity and microrotation fields while lowering the viscosity of the species mass boundary layer.

Keywords and phrases: Micropolar liquid, Chemical reaction, Inclined sheet, Porous medium Thermophoresis
2010 Mathematical Subject Classification: 65K05 , 90C06, 90C52, 90C56, 49M30

1. INTRODUCTION

The analysis of joint heat and mass diffusion is prominent in science, engineering and manufacturing activities due to huge applications

Received by the editors September 07, 2021; Revised: November 25, 2021; Accepted: December 14, 2021
www.nigerianmathematicalsociety.org; Journal available online at https://ojs.ictp.it/jnms/
[1]Corresponding author

derivable from such a study, for instance, in gas turbines, satellites and space vehicles, nuclear plants, electric transformers, etc. Many transport phenomena occur naturally and industrially where heat and mass transfer take place simultaneously by virtue of joint buoyancy influences of both heat transfer and species mass diffusion. These processes are encountered industrially in areas such as: food processing, crop damage due to freezing, polymer production, etc. [1-4].

The flow of fluids in a porous medium is consequential in different areas of science and technology due to its various relevance such as in spreading of chemical pollutants in saturated soil, ground water hydrology, irrigation systems, and in biomedical engineering such as, drug delivery and tissue implant. To this end, Nayak *et al.* [5] computationally offered the transfer of a reactive nanoliquid past a stretchable surface in permeable media. The authors narrated that the porous matrix offered a resistance force to the fluid flow whereas the thermal and solutal fields are enhanced by it. Olajuwon *et al.* [6] applied perturbation method to study such a phenomenon and showed that both Darcy and inertia parameters caused a decline in the velocity field. They stressed further that the temperature distribution may be altered by the impact of heat sink/generation and thus affect the flow field. More so, due to an extensive applications of studies that involved the impact of chemical reactions as found in hydrometallurgical and science of reacting species that includes, drying processes, food production, production of ceramics and polymers, etc., a number of researchers has investigated such phenomenon. For instance, Mohamed and Abo-Dahab [7] numerically discussed the radiating heat and reactive micropolar MHD flowing liquid along a vertical sheet which is being influenced by heat generation. Das *et al.* [8] scrutinized the impact of various parameters of the flowing reactive Casson liquid configured in permeable device. Mishra *et al.* [3] similarly offered a numerical report on the problem of MHD reactive micropolar flowing liquid with the inclusion thermo-diffusion along an impermeable stretching sheet whereas Fatunmbi and Odesola [9] considered such a system for unvarying thermal flux while Mishra *et al.* [10] addressed such a concept for a flowing micropolar liquid passing a semi-infinite flat sheet for the impact of radiation associated with constant heat source and magnetic field. The authors reported that the flow rate field rises for an enhancing values of microinertia term while the temperature field declines for a rising in both magnetic and porous terms in the presence/absence of heat source.

The thermophoresis concept is a phenomenon that usually occur when the force of temperature gradient act on the mixtures of mobile particles such that the various particles display different reactions to that force. In other words, this phenomenon relates to the transfer of colloidal particles due to varying temperature. The occurrence of gas thermal gradient stimulates the various unmixed particles to move towards the axis of low heat energy. This concept is commonly observed in the darkening of the shade of a kerosene lantern, during the combustion processes, the generated carbon particles are found to settle on the shade due to temperature gradient [11-12]. Such concept finds application in the control of micro-contamination, aerosol collection, gas streams removal of particles, etc [12-13]. In the initial study of such phenomenon, Goldsmith and May [14] explored the possibility of one-dimensional thermophoretic transport flow. Thereafter, various investigators [15-17] have improved on the subject by investigating the effect of diverse parameters under various configurations, assumptions and methods. None of these researchers however, has investigated such phenomenon on the non-Newtonian micropolar fluid inspite of its huge applications.

The concept of micropolar fluid consists of fluids with microstructures and rigid bar-like particles. Due to inherent microstructural features of micropolar fluids, they offer good mathematical framework in modelling and simulating complex and complicated fluids that could not be explained by the Navier-Stokes model (Newtonian model). Liquids that described micropolar formulation can be seen in: gas streams, exotic lubricants, colloids, animal blood and so on [18-19]. The theory of micropolar fluid as well as that of thermo-micropolar fluid was initiated by Eringen [20-21]. This model enables the coupling of microrotation and macro-velocity fields thereby displaying some microscopic effect leading to both translation and rotation of the fluid element. The flow analysis of some fluids such as: liquid crystals, blood flows, suspension solutions and various biological flows are the possible model for micropolar fluid [22]. There exists significant applications of such fluids in industrial activities and engineering such as, cap knee dynamics, blood arterial flows, synovial lubrication, slurry technologies, polymer extrusion, chemical science, bio-mechanic, a few of many [23-24].

Moreso, investigations of heat and mass transfer over various configurations with the application of non-Newtonian micropolar fluid have consequential relevance in biomedical and engineering activities such as in blood flows and dialysis, fluid flow in brain, flow in oxygenation, porous pipe design, design of filter [6, 23]. In view of these usefulness, several authors [1, 25-27] have investigated such studies with various parameters of interest, boundary conditions and assumptions.

Particularly, considering the immense applications of studies involving thermal and species distribution under the impact of thermophoresis and reacting species, it is worthwhile to investigate such a problem. However, in all studies above, the effects of thermophoresis along with viscous dissipation and non-uniform heat source have been ignored. Hence, this study aims to fill such a gap. Thus, this article examines non-Newtonian thermophoretic flow micropolar liquid passing an inclined sheet in permeable channel being characterized by reacting species, thermal dissipation and varying thermal absorption/generation effects. This research can be possibly applied in bio-technology such as drug distribution and tissue implant and other technological areas such as in extraction of crude oil, hydrology underground water, irrigation system, etc. A consistent and unconditionally stable shooting technique alongside Runge-Kutta-Fehlberg integration algorithm is adopted in this study. It is remarked that, in the absence of the porous medium, non-Newtonian micropolar fluid, microrotation vector, vortex viscosity and Darcy dissipation, the present investigation coincides with that of [17]. Hence, in such limiting situations, we have observed a good relationship between the report given by [17] and the references there-in with the present study.

2. MATHEMATICAL ANALYSIS & FORMULATION

Considering a convective reacting magneto-micropolar steadily flowing liquid on a two-dimensional semi-infinite inclined sheet in a porous medium as showcased in Fig. 1. The inclined surface is at an angle φ to the vertical, the x direction magnitude is coordinated in the axis plate with y in perpendicular direction, with the assumption that induced magnetic field is ignored, an unvarying magnetic field B_0 is used normal to the stream axis while suction is also imposed at the sheet surface. The transfer of heat is being influenced by viscous dissipation, varying heat source/sink (see equation 6), thermophoresis (see equation 7-8) while the flow characteristics have been taken to be uniform in nature apart from the density variation in buoyancy terms found in equation (2) which is approximated via Oberbeck-Boussinesq approximation.

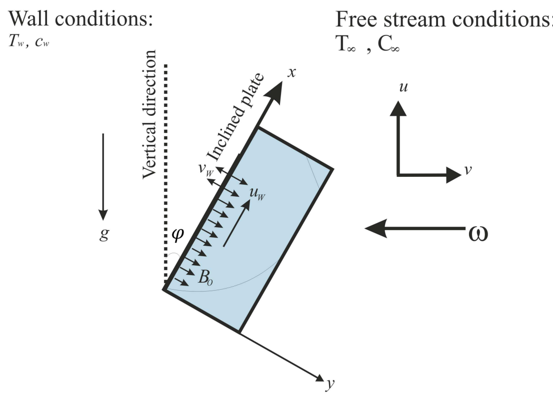

Fig. 1 The Geometry of the Physical Model

In view of the aforementioned coupled with Oberbeck-Boussinesq approximation, the modelled equations presented an extension of the studies by ([17, 29]:

$$\frac{\partial u}{\partial x}+\frac{\partial v}{\partial y}=0, \tag{1}$$

$$\rho\left(u\frac{\partial u}{\partial x}+v\frac{\partial u}{\partial y}\right)=(\mu+r)\frac{\partial^2 u}{\partial y^2}+r\frac{\partial B}{\partial y}+g\rho\beta_T\left(T-T_\infty\right)cos\varphi+$$
$$g\rho\beta_C\left(C-C_\infty\right)cos\varphi-\sigma B_0^2u-\frac{\mu}{k_p}u, \tag{2}$$

$$\rho j\left(u\frac{\partial B}{\partial x}+v\frac{\partial B}{\partial y}\right)=A\frac{\partial^2 B}{\partial y^2}-r\left(2B+\frac{\partial u}{\partial y}\right), \tag{3}$$

$$\rho c_p\left(u\frac{\partial T}{\partial x}+v\frac{\partial T}{\partial y}\right)=\kappa\frac{\partial^2 T}{\partial y^2}+(\mu+r)\left(\frac{\partial u}{\partial y}\right)^2+\sigma B^2u^2+$$
$$\frac{\mu}{k_p}u^2+q'''+\frac{DmK_T}{Cs}\frac{\partial^2 C}{\partial \bar{y}^2}, \tag{4}$$

$$u\frac{\partial C}{\partial \bar{y}}+v\frac{\partial C}{\partial y}=D_m\frac{\partial^2 C}{\partial y^2}+\frac{DmK_T}{T_m}\frac{\partial^2 T}{\partial y^2}-k_r\left(C-C_\infty\right)-\frac{\partial}{\partial y}\left(V_TC\right). \tag{5}$$

With q''' in equation (4) presented as (see [30-31])

$$q'''=\frac{\kappa U_0}{2x\nu}\left[\left(T_w-T_\infty\right)\left(\alpha e^{-\eta}+\beta\theta\right)\right], \tag{6}$$

The thermophoretic velocity V_T in equation (5) is written as:

$$V_T = -\frac{k_t^\star}{T_{ref}}\frac{\partial T}{\partial y}, \tag{7}$$

and the thermophoresis coefficient $k_t^\star$ is defined to be

$$k_t^\star = \frac{2Cs\left(\kappa/k_s + C_t K_n\right)\left(C_1 + C_2 e^{C_3/K_n}\right)}{\left(1 + 3C_m K_n\right)\left(1 + 2\kappa/k_s + 2C_t K_n\right)}. \tag{8}$$

The associated conditions at the boundary are:

$$\begin{aligned} &u = U_0, v = V_w, B = -s\frac{\partial u}{\partial y}, T = T_w, C = C_w \ at\ y = 0,\\ &u = 0, \omega \longrightarrow 0, T \longrightarrow T_\infty, C \longrightarrow C_\infty \text{ as } y \to \infty. \end{aligned} \tag{9}$$

From the governing equations (1-5), the component velocities are given respectively as u and v in x and y axis, μ denotes dynamic viscosity while ν denotes kinematic viscosity with κ symbolizing thermal conductivity, ρ stands for the liquid density whereas the vortex viscosity is denoted by r while j symbolizes micro-inertial density, c_p symbolizes constant pressure thermal capacity and A connotes the spin gradient viscosity. Similarly, T, T_w, T_∞ and B correspond to fluid temperature, sheet and free stream temperature, microrotation component in that order.

The suction/injection term is denoted by V_w, σ is the electrical conductivity while $\beta_T, \beta_C, k_r, k_p, D_m, Cs$ and T_m describe heat coefficient expansivity, species expansivity coefficient, reacting species rate, porous permeability of the device, mass diffusivity, fluid susceptibility and mean fluid temperature in that order.

Meanwhile, β and α symbolize heat generation/sink and space respectively, $C_1 ... C_3, C_m$ and C_t are constants while k_s represents the diffused particles thermal conductivity whereas the Knudsen number is given as K_n. Typical value of τ are 0.01, 0.05 and 0.1 correspondingly satisfying the values of $-k_t^\star\left(T_w - T_\infty\right)$ given rise to $3K, 15K$ and $30K$ for $T_{ref} = 300K$.

The parameter s in equation (9) stands for micropolar surface concentration parameter such that $0 \leq s \leq 1$. The case $s = 0$ depicts $B = 0$ as described by Jena and Mathur [32], it is a condition of strong microparticles species at the wall where the microparticles near the surface is incapable of rotation or translation. Meanwhile, Ahmadi [33] discussed a situation of weak concentration such that effect of microrotation influence becomes negligible in the neighbourhood of the boundary, in this case, $s = 1/2$ becomes relevant. However, $s = 1$ is applicable for turbulent

boundary layer situations as opined by Peddieson [34]. The level at which micropolar liquid deviates from the viscoplastic classical material concept may be discovered by the viscosity vortex size term r, therefore, with $r = 0$, then equation (3) is dissociated from equations (2) and (4), as a result, the formulation addressed in this study as well as the outcomes gotten corresponds to the Newtonian liquid formulation. In line with previous authors ([16-17, 37]) and to obtain a pure similarity solution, the following terms have been assumed to be proportional to x: $V_w = V_0 x^{-1/2}$, $\sigma = \sigma_0 x^{-1}, \beta_T = \beta_0 x^{-1}, \beta_C = \beta_0^{\star} x^{-1}, k_r = k_1 x^{-1}, k_p = k_0 x$ where $V_0, \sigma_0, \beta_0, \beta_0^{\star}, k_1$ and k_0 are constants.
The dimensionless quantities in equation (10) are introduced into the governing equations (1-8).

$$\begin{aligned}&\eta = y\left(\frac{U_0}{2x\nu}\right)^{1/2},\ \psi = \left(2U_0 x\nu\right)^{1/2} f(\eta),\ B = U_0\left(\frac{U_0}{2x\nu}\right)^{1/2} g(\eta),\\ &A = \left(\mu + \frac{r}{2}\right) j,\ j = \frac{\nu x}{U_0}, \phi(\eta) = \frac{C - C_\infty}{C_w - C_\infty},\ \theta(\eta) = \frac{T - T_\infty}{T_w - T_\infty},\\ &u = \frac{\partial \psi}{\partial y}, v = -\frac{\partial \psi}{\partial x}.\end{aligned} \tag{10}$$

The use of quantities (10) ensures the validity of equation (1). Taking cognizance of equations (6-8) and using (10) equations (2-5) therefore translate to:

$$(1+K)\, f''' - [Da + M]\, f' + K g' + f f'' + Gr\theta\cos\varphi + Gc\phi\cos\varphi = 0, \tag{11}$$

$$\left(1 + \frac{K}{2}\right) g'' - 2K\left(2g + f''\right) + \left(f'g + fg'\right) = 0, \tag{12}$$

$$\begin{aligned}&\theta'' + Pr\left[f\theta' + (1+K)\, Ecf''^2 + Ec\,(M + Da)\, f'^2 + PrDu\phi''\right] +\\ &\left(\alpha e^{-\eta} + \beta\theta\right) = 0,\end{aligned} \tag{13}$$

$$\phi'' - Sc\left[\zeta\phi - \left(f - \tau\theta'\right)\phi' - \left(Sr - \tau\phi\right)\theta''\right] = 0, \tag{14}$$

the conditions at the boundary also become:

$$\begin{aligned}&f'(0) = 1,\ f(0) = fw,\ g(0) = -sf'',\ \theta(0) = 1,\ \phi(0) = 1\\ &f'(\infty) = 0\ g(\infty) = 0,\ \theta(\infty) = 0,\ \phi(\infty) = 0.\end{aligned} \tag{15}$$

With

$$\begin{aligned} fw &= \frac{-\sqrt{2}V_0}{\left(\sqrt{U_0 \nu}\right)}, M = \frac{2\sigma_0 B_o^2}{\rho U_0}, Gr = \frac{2g\beta_0\left(T_w - T_\infty\right)}{U_0^2}, \zeta = \frac{2k_1}{U_0}, \\ Gc &= \frac{2g\beta_0^\star\left(C_w - C_\infty\right)}{U_0^2}, K = \frac{r}{\mu}, Ec = \frac{U_0^2}{cp\left(T_w - T_\infty\right)}, \\ Da &= \frac{2\nu}{k_o U_0}, Sc = \frac{\nu}{Dm}, Du = \frac{D_m K_T (C_w - C_\infty)}{Csc_p \nu (T_w - T_\infty)}, \\ Sr &= \frac{DmK_T\left(T_w - T_\infty\right)}{T_m \nu\left(C_w - C_\infty\right)}, \tau = -\frac{k_t^\star\left(T_w - T_\infty\right)}{T_{ref}}, Pr = \frac{\mu c_p}{\kappa}. \end{aligned} \tag{16}$$

For engineering purposes, the essential variables of fascinating include the wall coefficient friction as well as thermal gradient and Sherwood number which are orderly described in equation (17) as

$$\begin{aligned} &C_{fx} = \tau_w (\rho u_w^2)^{-1},\ Nu_x = xq_w[\kappa\left(T_w - T_\infty\right)]^{-1}, \\ &Sh_x = xq_m[D_m\left(C_w - C_\infty\right)]^{-1}, \end{aligned} \tag{17}$$

with τ_w being shear stress, q_w thermal flux at the wall, meanwhile, q_m indicating the species flux at the plate wall such that

$$\tau_w = \left[(\mu + r)\frac{\partial u}{\partial y} + rB\right]_{y=0},\ q_w = -\left[\kappa\frac{\partial T}{\partial y}\right]_{y=0}, q_m = -\left[Dm\frac{\partial C}{\partial y}\right]_{y=0} \tag{18}$$

upon substituting (10) and (18) in (17), the skin friction coefficient yields

$$C_{fx} = \left[1 + (1 - s)\, K\right] Re_x^{-1/2} f''(0), \tag{19}$$

whereas the thermal gradient and concentration gradient respectively transform to

$$Nu_x = -Re_x^{1/2}\theta'(0), Sh_x = -Re_x^{1/2}\phi'(0) \tag{20}$$

3. METHOD OF SOLUTION

The equations (11-14) together with (15) constitutes highly nonlinear equations which the closed form analytical solution is not feasible. Thus, in this study, numerical solution has been sought by means shooting scheme in company with integrating Runge-Kutta-Fehlberg. By this approach, an appropriate definite $\eta \to \infty$ value has been chosen (say η_∞) and the governing equations (11-14) are translated into a system of first-ninth order simultaneous linear equations and thereafter reduced into an initial value problem (IVP). For details on the shooting technique (see [38-39]). However,

to solve this set of equations as an IVP requires nine initial solution conditions but only five are available. To start the process of solution therefore, some initial guess are selected for the unknown initial conditions h_1, h_2, h_3 and h_4 which correspond to $\phi'(0)$, $\theta'(0)$, $g'(0)$ and $f''(0)$. This process is done repeatedly with a larger η_∞ and continues until the successive outcome values for the unknown initial conditions $\phi'(0)$, $\theta'(0)$, $g'(0)$ and $f''(0)$ gives a difference for a noteworthy satisfying digit. Hence, the final η_∞ value is then selected as appropriate value of the limit η_∞ for some fluid controlling terms. The higher order equations have been translated into first order equations as follows:
Let

$$r_1 = f, r_2 = f', r_3 = f'', r_4 = g, r_5 = g', r_6 = \theta,$$
$$r_7 = \theta', r_8 = \phi, r_9 = \phi' \tag{21}$$

$$r_3' = -\left[\frac{Kr_5 + r_1r_3 + Gr\ r_6cos\varphi + Gc\ r_8\varphi + (Da + M)r_2}{(1+K)}\right], \tag{22}$$

$$r_5' = \frac{2K(2r_4 + r_3) - (r_1r_4 + r_1r_5)}{(1 + K/2)}, \tag{23}$$

$$r_7' = -\left[Pr\ r_1r_7 + (1+K)\ Pr\ Ec\ r_3 + Pr\ Ec\ (M + Da)\ r_2 + (\alpha e^{-\eta} + \beta\ r_6) + PrDu\ r_9'\right], \tag{24}$$

$$r_9' = Sc\ \zeta\ r_8 - Sc(Sr - \tau\ r_8)r_7' - Sc(r_1 - \tau\ r_7)r_8, \tag{25}$$

with the boundary conditions given as

$$\begin{aligned} &r_1(0) = 0, r_2(0) = 1, r_3(0) = h_1, r_4(0) = -sf_3(0), r_5(0) = h_2,\\ &r_6(0) = 1, r_7(0) = h_3, r_8(0) = 1, r_9(0) = h_4, r_2(\infty) \to 0,\\ &r_4(\infty) \to 0, r_6(\infty) =\to 0, r_8(\infty) =\to 0 \end{aligned} \tag{26}$$

When all the initial conditions have been obtained, a computer algebra symbolic package (Maple 2016) is adopted for the resulted equations.

4. ANALYSIS OF RESULTS AND DISCUSSION

The trends of the emerging parameters listed in (16) on the flow profiles and on the coefficient of wall friction C_{fx}, thermal gradient Nu_x and mass gradient Sh_x are analyzed in this section using graphs. Firstly, the accuracy and authenticity of the computed code employed have been verified by comparing the results obtained in this study relating to C_{f_x} and Nu_x with the Chebyshev collocation method and Runge-Kutta method as respectively given by [28] and

[17] in the absence of $K, \tau, \alpha, \beta, \zeta, \varphi, Ec$ and Da. These comparisons are offered in Table 1 and seen to be in good alliance with existing reports.
The computational default values used for the analysis in the current study are $K = 2.0, M = 0.5, Gr = 6.0, Gc = 4.0, Du = 0.6, Sr = 0.2, Ec = 0.2, \alpha = 0.2, \beta = -0.5, Pr = 0.71, Sc = 0.62, r = Da = fw = 0.5, \varphi = \Pi/3, \tau = 0.2, \zeta = 2.0$. Unless stated otherwise in various plots.

Table 1: Computed values of C_{f_x} and Nu_x as compared with [28] and [17]

Du	Sr	[28]		[17]		Present	
		C_{fx}	Nu_x	C_{fx}	Nu_x	C_{fx}	Nu_x
0.030	2.0	6.2285	1.1565	6.238707	1.151932	6.229908	1.156453
0.037	1.6	6.1491	1.1501	6.160867	1.144651	6.150610	1.150059
0.050	1.2	6.0720	1.1428	6.087934	1.135752	6.073556	1.142710
0.075	0.8	6.0006	1.1333	6.023187	1.123219	6.002251	1.133220
0.150	0.4	5.9553	1.1157	5.996934	1.096560	5.957028	1.115613

The variations in the material parameter K and the magnetic field term M on the flow field, temperature and microrotation fields are depicted in Figures 2a, 2b and 3a in that order. For figure 2a, the velocity reaches the maximum point near the inclined sheet and then descended asymptotically to the up stream condition. At a distance $\eta \approx 1.5$ away from the sheet, there is an intersection of the profiles such that the trend is reversed as K continues to rise in magnitude, an increase in the fluid stream distribution is observed. This pattern is due to the dominance of the vortex viscosity over that of the dynamic viscosity as K advances. However, with advancement in the profile of M, a reducing motion takes place in the velocity field as observed in figure 2a. This behaviour corresponds to the action of the resistive force (electromagnetic force) created by the imposition of the transverse magnetic field to the micropolar conducting liquid. Thus, as M appreciates in strength, the fluid motion is resisted and lowered. Consequent upon the fluid locomotive resistance produced by the Lorentz force as M grows, the temperature distribution is enhanced due to higher friction between the fluid and the sheet as portrayed in Figure 2b. In the same behaviour, the micropolar fluid temperature is found to appreciate with rising values of the material term K.

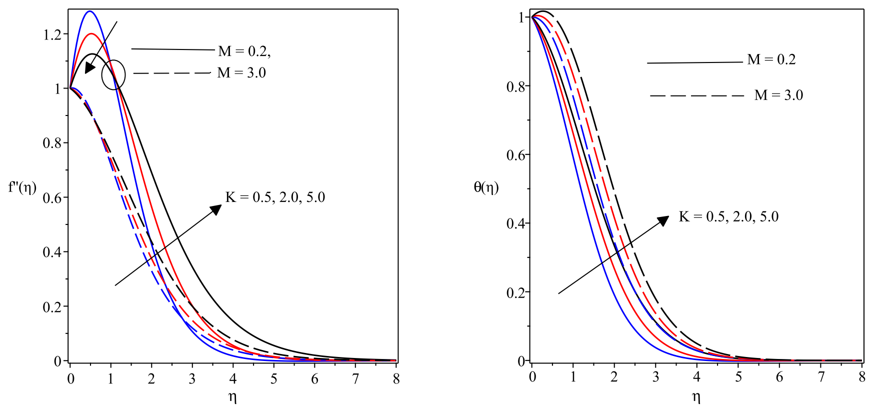

a **b**

Figure 2: Variation of micropolar material K and magnetic term M on (a) velocity profiles and (b) temperature fields.

The microrotation profile rises for a rising in both K and M values as presented in Figure 3a with a reverse microparticles rotation for a hike in K. The influence of thermal Grashof number Gr is to boost the liquid motion as depicted in Figure 3b. Physically, Gr describes the buoyancy relation to the force of viscous, hence, growing values of Gr encourages the pressure gradient causing the fluid motion to advance. Conversely, increasing values of Darcy term Da leads to a decline in the momentum boundary layer, thereby, lowering the fluid locomotion as displayed Figure 3b.

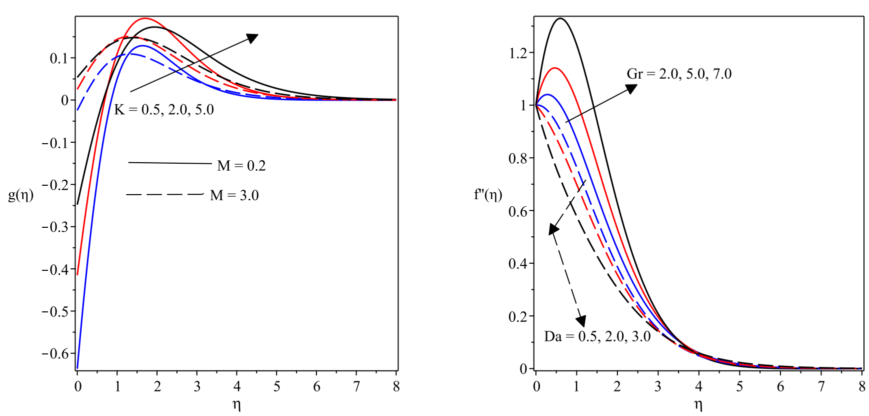

a **b**

Figure 3: Variation of micropolar material K and magnetic term Gr on (a) micropolar profiles and (b) elocity fields.

Figure 4a portrays the reaction of the thermal profile to a change in Prandtl number Pr and space heat generation term $\alpha > 0$. Basically, Pr describes the rate at which thermal diffusion occurs as compared to momentum diffusion, an enhance in Pr propels the temperature boundary viscosity structure to decline and consequently lower the temperature distribution. On this premise, the Prandtl number may be employed to enhance the cooling rate of fluids. On the contrary, the temperature is seen as an increasing function of the space-dependent heat source α as illustrated also in Figure 4a. This trend is due to a rise in α leads to production of more heat thereby causing the micropolar fluid temperature to escalate. Figure 4b is a graph of the fluid heat versus η for varying values of Eckert number Ec and heat absorption term $\beta < 0$. Growing values of Ec causes an advancement in the temperature profiles owing to an additional heat generated by the frictional drag of the fluid particles whereas the opposite is the case for the heat absorption parameter $\beta < 0$ by virtue of a fall in the thickness of the temperature boundary viscid with a growth in the heat absorption term.

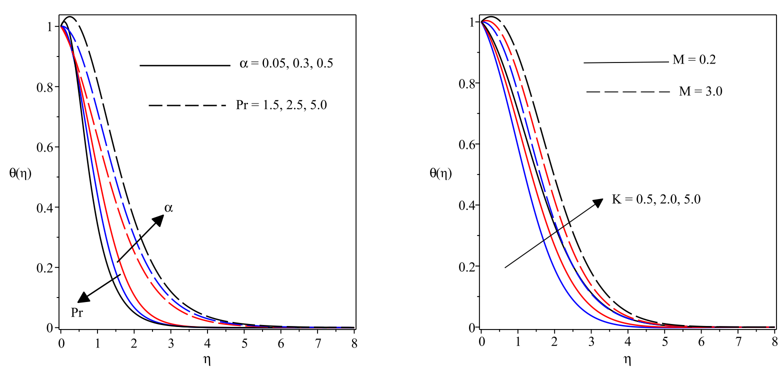

a **b**

Figure 4: Response of temperature profiles to variation in (a) Prandtl number Pr & $\alpha > 0$ (b) Eckert number Ec & $\beta < 0$

Figure 5a describes the graph of the concentration field versus η for changes that occur in the reacting species term ζ in the presence of the Schmidt number Sc. The Schmidt number Sc physically describes the viscosity of the flow velocity and concentration boundary thickness and at such, it is proportionally inverse to the species diffusion. Thus, an uplift in Sc compels a decline in the mass diffusivity and resulted to a decrease in the mass profiles. In a related sense, the growth in the magnitudes of the chemical reaction term ζ also causes a decrease in the mass transport profile as a result of a thin solutal boundary layer structure. Here, a rise in ζ depicts an increase in the reacting degenerative species along the species dissolves efficiently as a result, the concentration field is lowered. In the same vein, Figure 5b demonstrates that the influence of the thermophoresis term τ is to dampen the structure of the boundary layer and consequently lower the concentration profiles.

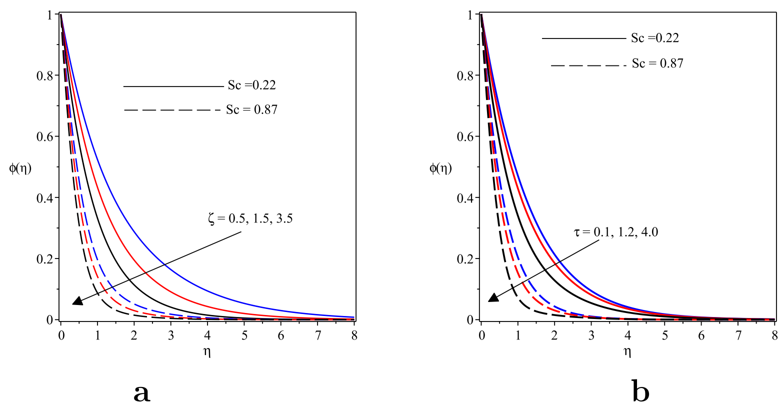

Figure 5: Mass species propagation for various values of (a) chemical reactive ζ & Schmidt Sc terms (b) thermophoresis τ & Schmidt Sc parameters.

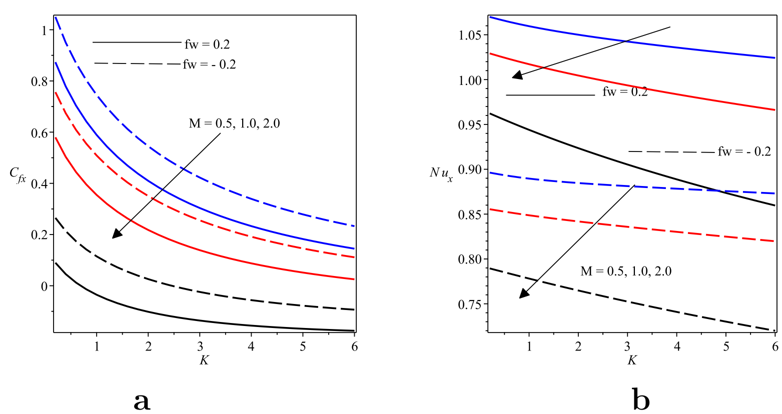

Figure 6: Combined impact of material K and magnetic field parameters M on (a) the wall coefficient friction C_{fx} and (b) on heat gradient Nu_x

It is conspicuously noticed in Figure 6a that both the magnetic term M and the material micropolar term K act to reduce the wall coefficient friction C_{fx} in the occurrence of both injection ($fw < 0$) and suction ($fw > 0$) terms. However, the existence of injection is less than the suction, C_{fx} as noticed in this case. It is noted that the viscous drag can be reduced by fluids with microstructures and rigid bar-like particles such as the micropolar liquid. In the same way, the response of the thermal gradient Nu_x as observed in Figure 6b is similar to that of C_{fx} that is, Nu_x reduces with growing values of both M and K. However, the heat transport at the sheet improves better for suction than that of injection. The reactions from these figures imply that suction/injection can be applied for stabilizing the boundary layer growth.

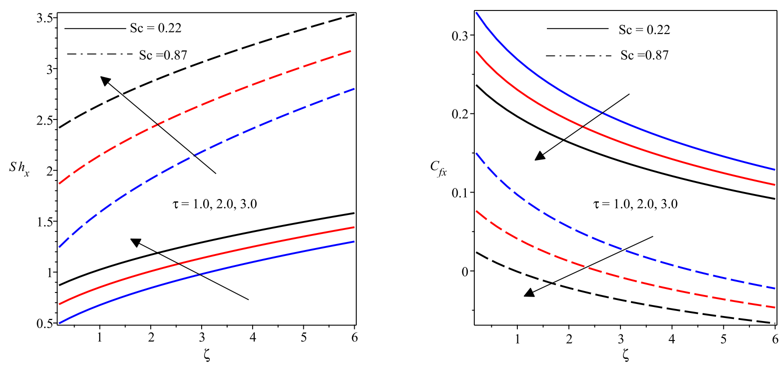

a **b**

Figure 7: Combined impact of Schmidt number Sc, chemical reaction ζ and thermophoresis τ parameters on (a) Sherwood number and (b) skin friction coefficient C_{fx}.

Figures 7a and 7b describe the plots of the Sherwood number Sh_x against ζ for variation in the thermophoresis parameter τ when Schmidt number Sc is present. Revelation here points to the fact the mass transfer is enhanced by increasing thermophoresis term τ, likewise, for any chosen value of τ an increase ζ facilitates a rise in Sh_x. However, in these cases, the Sherwood number Sh_x improves better for higher values Schmidt number Sc as noticed in Figure 7a. Increasing values of τ has a declining influence on C_{fx} as depicted in Figure 7b, in the like manner, an increase in ζ for any fixed value of τ and Sc also dampen C_{fx}.

Figure 8a depicts a plot of Nu_x versus ζ for changes in τ in the presence of Sc. Clearly, the thermal gradient Nu_x is a reducing function of both τ and ζ as well as Sc as evidenced in this figure. The implication is that the heat transfer declines with a rise in magnitude of these parameters. Figure 8b informs that the mass transfer advances with enhancing Dufour number Du (or reducing Soret Sr) in the absence of the thermophoretic term τ whereas the opposite is the case in the presence of τ.

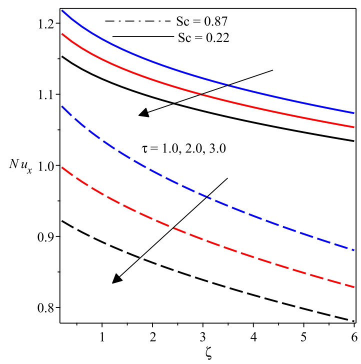

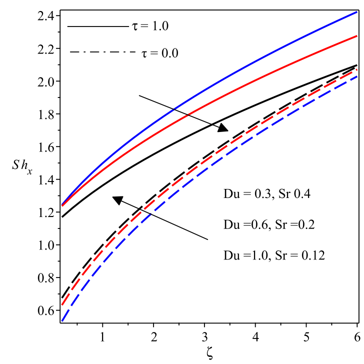

a **b**

Figure 8 Combined effects of (a) thermophoresis τ, chemical reaction ζ and Schmidt number Sc on Nu_x (b) Dufour(Soret) Du/Sr, thermophoresis τ and chemical reaction parameter ζ on Sh_x.

4. CONCLUDING REMARKS

This research study theoretically investigated the flow as well as thermal and species transport of thermophoretic magneto-micropolar reactive liquid configured in an inclined two-dimensional sheet in a porous enclosure. The stream field is impacted by vary heat generation/absorption, buoyancy forces, viscous dissipation as well as Soret-Dufour effects. The modelled equations have been numerically integrated by means of Fehlberg-Runge-Kutta technique in together with shooting technique. The outcomes gotten in the study have been examined with earlier reported results in literature as special cases of the current study and found to be in good relationship. Various graphs have been constructed to portray the impact of the main controlling terms on the non-dimensional quantities. From this analysis, the following points were deduced.

- The motion of fluid flow reduces with imposition of the magnetic field M and Darcy Da parameters whereas it rises with rising values of the buoyancy force Gr and material (micropolar) K terms.
- The mass transfer appreciates with growing thermophoresis term values τ and Schmidt number Sc whereas both parameters act to lower the skin friction coefficient C_{fx}.
- The presence of the microstructure particles and the magnetic field parameter facilitate the reduction of the viscous drag stress C_{fx} and the heat transfer rate Nu_x across the boundary layer.

- An increment in the magnitudes of Ec, α, M and K lead to the growth in the viscosity of the temperature boundary layer while an inverse behaviour is seen for rising magnitude of Pr and $\beta < 0$.
- The growth in magnitudes of the chemical reaction ζ, Schmidt number Sc as well as thermophoresis parameters τ tend to lower the viscosity of the mass boundary layer and consequently reduce the chemical reacting distribution.

ACKNOWLEDGEMENTS

The author would like to thank the anonymous referee whose comments improved the original version of this manuscript.

NOMENCLATURE

x, y: Cartesian coordinates $[m]$
u, $\bar{v}$: Velocity components $[ms^{-1}]$
B: Microrotation component $[s^{-1}]$
T: Fluid temperature $[K]$
C: Species concentration $[molm^{-}3]$
C_w: Species concentration at the sheet $[molm^{-}3]$
C_∞: Free stream species concentration $[molm^{-}3]$
T_w: Fluid temperature at wall $[K]$
T_∞: Free stream temperature $[K]$
T_m: Mean fluid temperature $[K]$
r: Vortex viscosity $[kgm^{-1}s^{-1}]$
g: Acceleration due to gravity $[ms^{-2}]$
D_m: mass diffusivity $[m^2s^{-1}]$
q''': Non-uniform heat source/sink $[Wm^{-3}K^{-1}]$
k_r: Constant rate of chemical reaction $[Mol/s]$
k_p: Permeability of the porous media $[m^2]$
v_w: Suction/injection velocity $[ms^{-1}]$
B_0: Magnetic field strength $[A/m]$
j: Micro-inertia per unit mass $[m^2]$
q_w: Heat flux at the surface of the plate $[Wm^{-2}]$
A: Spin gradient viscosity $[m^2s^{-1}]$
c_p: Specific heat at constant pressure $[J/kgK]$
q_w: Heat flux at the surface $[Wm^{-2}]$
q_m: Mass flux at surface $[Wm^{-2}]$
f: Dimensionless stream function
K: Material parameter

Gr: Thermal Grashof number
Gc: Solutal Grashof number
Pr: Prandtl number
Sc: Schmidt number
fw: Suction/injection parameter
Ec: Eckert number
Da: Darcy number
Fs: Forchheimer number
Du: Dufour number
Sr: Soret number
M: Magnetic field parameter
C_{f_x}: dimensionless local skin friction coefficient
Nu_x Dimensionless local Nusselt number(rate of heat transfer at the surface)
Sh_x Dimensionless local Sherwood number (rate of mass transfer at the surface)
φ: Angle of inclination $[rad]$
κ: Thermal conductivity coefficient $[Wm^{-1}K^{-1}]$
ρ: Density of the fluid $[kgm^{-3}]$
ψ: Stream function $[m^2s^{-1}]$
σ: Electric conductivity $[Sm^{-1}]$
μ: Dynamic viscosity $[kgm^{-1}s^{-1}]$
ν: Kinematic viscosity $[m^2s^{-1}]$
β_T: Coefficient of thermal expansion $[K^{-1}]$
β_C: Coefficient of concentration expansion $[K^{-1}]$
η: Dimensionless scaling transformation variable
ζ: Chemical reaction parameter
τ: Thermophoresis parameter
$\theta(\eta)$: Dimensionless temperature
$\phi(\eta)$: Dimensionless species concentration

References

[1] E. O. Fatunmbi, H. A. Ogunseye, and P. Sibanda, *Magnetohydrodynamic micropolar fluid flow in a porous medium with multiple slip conditions*, International Communication in Heat and Mass Transfer, **115** 1-10, 2020.

[2] Y. Varol, H. Oztop, F. and Varol, *Natural convection in porous triangular enclosures with a solid adiabatic fin attached to the horizontal wall*, International Communication in Heat and Mass Transfer, **34**(1), 19-27, 2007.

[3] S. R. Mishra, S. Baag and D. K. Mohapatra, *Chemical reaction and Soret effects on hydro magnetic micropolar fluid along a stretching sheet*, Engineering Science and Technology, an International Journal, **19** 1919-1928, 2016.

[4] M. S. Astanina, M. A. Sheremet, H. F. Oztop and N. Abu-Hamdeh, *MHD natural convection and entropy generation of ferrofluid in an open trapezoidal cavity partially filled with a porous medium*, International Journal of Mechanical Science, **48** 1841-1853, 2018.

[5] M. K. Nayaka, S. Shaw and O. D. Makinde, *Chemically reacting and radiating nanofluid flow past an exponentially stretching sheet in a porous medium*, Indian Journal of Pure and Applied Physics, **56** 773-786, 2018.

[6] B. I. Olajuwon, J. I. Oahimire and M. A. Waheed, *Convection heat and mass transfer in a hydromagnetic flow of a micropolar fluid over a porous medium*, Theoret.Appl.Mech., **41**(2) 93-117, 2014.

[7] R. A. Mohamed and S. M. Abo-Dahab, *Influence of chemical reaction and thermal radiation on the heat and mass transfer in MHD micropolar flow over a vertical moving porous plate in a porous medium with heat generation*, International Journal of Thermal Sciences, **48**, 1800-1813, 2009.

[8] M. Das, G. Mahanta, S. Shaw, and S. B. Parida, *Unsteady MHD chemically reactive double?diffusive Casson fluid past a flat plate in porous medium with heat and mass transfer*, Heat Transfer-Asian Res, **48** 1761-1777, 2019.

[9] E. O. Fatunmbi, and A. S. Odesola, *MHD Free convective heat and mass transfer of a micropolar fluid flow over a stretching permeable sheet with constant heat and mass flux*, Asian Research Journal of Mathematics, **9**(3) 1-15, 2018.

[10] S. R. Mishra, M. M. Hoque, B. Mohanty and N. N. Anika, *Heat transfer effect on MHD flow of a micropolar fluid through porous medium with uniform heat source and radiation*, Nonlinear Engineering, **18** 1-9, 2018.

[11] L. Talbot, R. K. Cheng, R. W. Scheffer and D. P. Wills, *Thermophoresis of particles in a heated boundary layer*, J Fluid Mech, **101** 73-78, 1980.

[12] I. L. Animasaun, *Effects of thermophoresis, variable viscosity and thermal conductivity on free convective heat and mass transfer of non-darcian MHD dissipative Casson fluid flow with suction and nth order of chemical reaction*, Journal of Nigerian Mathematical Society, **34** 11-31, 2015.

[13] S. K. Parida, S. Panda and B. R. Rout, *MHD boundary layer slip flow and radiative nonlinear heat transfer over a flat plate with variable fluid properties and thermophoresis*, Alexandria Engineering Journal, **54** 941-953, 2015.

[14] P. Goldsmith and F. G. May, *Diffusiophoresis and thermophoresis in water vapour systems, in: Aerosol Science*, Academic Press, London, 1966.

[15] MD. Aurangzaib, S. Uddin, K. Bhattacharyya and S. Shafie, *Micropolar fluid flow and heat transfer over an exponentially permeable shrinking sheet*, Propulsion and Power, **32** 1-8, 2016.

[16] K. Das, S. Jana and P. K. Kundu, *Thermophoretic MHD Slip Flow over a permeable surface with variable fluid properties*, Alexandria Engineering Journal, **26** 35-44, 2015.

[17] H. Mondal, D. Pal, S. Chatterjee and P. Sibanda, *Thermophoresis and Soret-Dufour on MHD mixed convection mass transfer over an inclined plate with non-uniform heat source/sink and chemical reaction*, Ain Shams Engineering Journal, **57** 1-11, 2017.

[18] M. Qasim, I. Khan and S. Shafle, *Heat transfer in a micropolar fluid over a stretching sheet with Newtonian heating*, Plos One, **8**(4), 1-6, 2013.

[19] D. Srinivasacharya and U. Mendu, *Free convection in MHD micropolar fluid with radiation and chemical reaction effects*, Chem. Ind. Chem. Eng. **20**(2), 183-195, 2014.

[20] A. C. Eringen, *Theory of micropolar fluids*, J. Math. Anal. Appl., **16** 1-18, 1966.

[21] A. C. Eringen, *Theory of thermo-microfluids*, Journal of Mathematical Analysis and Applications, **38** 480-496, 1972.

[22] B. Mohanty, S. R. Mishra and H. B. Pattanayak, *Numerical investigation on heat and mass transfer effect of micropolar fluid over a stretching sheet through porous media*, Alexandria Engineering Journal, **54** 223-232, 2015.

[23] G. Lukaszewicz, *Micropolar fluids: Theory and Applications* (1st Ed.). Birkhauser Boston, **33** 1028-1031, 1999.

[24] U. Reena and S. Rana, *Effect of Dust Particles on rotating micropolar fluid heated from below saturating a porous medium*, Applications and Applied Mathematics: An International Journal, **4** 189-217, 2009.

[25] S. O. Salawu and E. O. Fatunmbi, *Dissipative heat transfer of micropolar hydromagnetic variable electric conductivity fluid past inclined plate with Joule heating and non-uniform heat generation*, Asian Journal of Physical and Chemical Sciences, **2**(1), 1-10, 2017.

[26] E. O. Fatunmbi and O. J. Fenuga, *MHD micropolar fluid flow over a permeable stretching sheet in the presence of variable viscosity and thermal conductivity with Soret and Dufour effects*, International Journal of Mathematical Analysis and Optimization: Theory and Applications, **17** 211-232, 2017.

[27] E. O. Fatunmbi, and A. Adeniyan, *MHD stagnation point-flow of micropolar fluids past a permeable stretching plate in porous media with thermal radiation, chemical reaction and viscous dissipation*, Journal of Advances in Mathematics and Computer Science, **26**(1), 1-19, 2018.

[28] M. S. Alam, M. Ferdows, M. Ota and M. A. Maleque, *Dufour and Soret effects on steady free convection and mass transfer flow past a semi-infinite vertical porous plate in a porous medium*, Int J Appl Mech Eng, **11**(3):535-545, 2008.

[29] E. O. Fatunmbi, S. S. Okoya and O. D. Makinde, *Convective heat transfer analysis of hydromagnetic micropolar fluid flow past an inclined nonlinear stretching sheet with variable thermo-physical properties*, Diffusion Foundations, **26** 63-77, 2020.

[30] D. Pal, and H. Mondal, *Effect of Soret Dufour chemical reaction and thermal radiation on MHD non-Darcy unsteady mixed convective heat and mass transfer over a stretching sheet*, Commun Nonlinear Sci Numer Simulat, **16** 1942-1958, 2014.

[31] M. M. Nandeppanavar, M. C. Kemparaju and S. Shakunthala, *MHD stagnation point slip flow due to a non-linearly moving surface with effect of non-uniform heat source*, Nonlinear Engineering, **18** 1-13, 2018.

[32] S. K. Jena and M. N. Mathur, *Similarity solutions for laminar free convection flow of a thermomicropolar fluid past a non-isothermal flat plate*, Int. J. Eng. Sci. **19** 1431-1439, 1981.

[33] G. Ahmadi, *Self-similar solution of incompressible micropolar boundary layer flow over a semi-infinite plate*, Int. J. Engng. Sci, **14** 639-646, 1976.

[34] J. Peddieson, *An application of the micropolar model to the calculation of a turbulent shear flow*, Int. J. Eng. Sci., **10** 23-32, 1972.

[35] A. Ishak, *Similarity solutions for flow and heat transfer over a permeable surface with convective boundary condition*, Applied Mathematics and Computation, **217** 837-842, 2010.

[36] O. D. Makinde, W. A. Khan and J. R. Culham, *MHD variable viscosity reacting flow over a convectively heated plate in a porous medium with thermophoresis and radiative heat transfer*, International Journal of Heat and Mass Transfer, **93** 595-604, 2016.

[37] M. M. Rahman, A. Aziz and M. A. Al-Lawatia, *Heat transfer in micropolar fluid along an inclined permeable plate with variable fluid properties*, Int. J of Thermal Sciences, **49** 993-1002, 2010.

[38] B. S. Attili and M. L. Syam, *Efficient shooting method for solving two point boundary value problems*, Chaos, Solitons and Fractals, **35** 895-903, 2008.

B. Mahanthesh, B. J. Gireesha, R. S. R. Gorla and O.D. Makinde, *Magnetohydrodynamic three-dimensional flow of nanofluids with slip and thermal radiation over a nonlinear stretching sheet: a numerical study*, Neural Comput & Applic, **30** 1557-1567, 2018.

DEPARTMENT OF MATHEMATICS AND STAATISTICS, FEDERAL POLYTECHNIC, ILARO, NIGERIA
E-mail address: olusojiephesus@yahoo.com

DEPARTMENT OF MATHEMATICS, LANDMARK UNIVERSITY, OMU-ARAN, NIGERIA
E-mail address: kunlesalawu2@gmail.com

DEPARTMENT OF MATHEMATICS, LAGOS STATE POLYTECHNIC, IKORODU, NIGERIA
E-mail address: joshua104u@yahoo.com